Superamphiphobic surfaces

Chu, Zonglin ; Seeger, Stefan

Abstract: Superamphiphobicity is an effect where surface roughness and surface chemistry combine to generate surfaces which are both superhydrophobic and superoleophobic, i.e., contact angles (yCA) greater than 1501 along with low contact angle hysteresis (CAH) not only towards probing water but also for low-surface- tension 'oils'. In this review, we summarize the research on superamphiphobic surfaces, including the characterization of superamphiphobicity, different techniques towards the fabrication of surface roughness and surface modification with low-surface-energy materials as well as their functional applications.

DOI: https://doi.org/10.1039/c3cs60415b

Superamphiphobic surfaces

Zonglin Chu and Stefan Seeger*

Received (in XXX, XXX) Xth XXXXXXXXX 20XX, Accepted Xth XXXXXXXXX 20XX
DOI: 10.1039/b000000x

Superamphiphobicity is an effect where surface roughness and surface chemistry combine to generate surfaces which are both superhydrophobic and superoleophobic, *i.e.*, contact angles (θ_{CA}) greater than 150° along with low contact angle hysteresis (CAH) not only towards probing water but also for low-surface-tension 'oils'. In this tutorial review, we summarize the research on superamphiphobic surfaces, including the characterization of superamphiphobicity, different techniques towards the fabrication of surface roughness and surface modification with low-surface-energy materials as well as their functional applications.

1. Introduction

Research on super-antiwetting and the observation of extremely high θ_{CA} dates back to more than a century ago—θ_{CA} nearly 180° was firstly achieved *via* coating a substrate with soot, reported by Ollvier in 1907.[1] Thereafter, super-antiwetting surface with water θ_{CA} higher than *ca.* 150° and sliding angle (θ_{SA}) lower than *ca.* 10°, which is now defined as a superhydrophobic surface, received continued but relatively limited interest until 1997 when the explanation of the origin and the universal principle of the 'lotus effect' in nature by Barthlott and Neinhuis.[2] They revealed that the epicuticular wax crystalloids on the surface (Fig. 1) are responsible for the superhydrophobicity and self-cleaning property. Taking the lotus leaf as an example, self-cleaning means that particles adhered to the surface can be removed easily while the droplet is rolling off. Therefore, self-cleaning is a common characteristic of superhydrophobic surfaces. Since then, research interest in superhydrophobicity has been motivated by mimicking nature, and thereby great effort was devoted to the understanding of the surface structures of different plants and animals, and therefore the fabrication of similar artificial materials.[3,4]

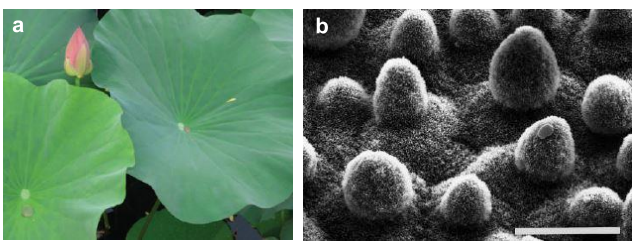

Fig. 1 Lotus leaves in nature: self-cleaning behaviour (a) and the related microstructures as observed by scanning electron microscopy, SEM (b). Scale bar = 20 μm. Fig. 1a was reproduced with permission from ref. 3. Fig. 1b was reproduced with permission from ref.2, copyright 1997 by Springer-Verlag Berlin/Heidelberg.

However, it remains a challenge to create superoleophobic surfaces that resist wetting for organic liquids because of their low surface tensions, for example, 23.8 $mN \cdot m^{-1}$ for decane, which are much lower than that of water (72.3 $mN \cdot m^{-1}$). To the best of our knowledge, superoleophobic surface was first developed through the design of re-entrant surface curvature, in conjunction with chemical composition and roughened texture surface, by Tuteja *et al.* in 2007.[5] Afterwards, it was well-recognized that the combination of appropriate surface roughness and materials with a low surface energy (mainly fluoro-derived compounds) is a successful way to prepare superoleophobic surfaces. Therefore, a variety of superoleophobic surfaces were reported continuously,[6–10] and the terminology 'superamphiphobic'[6,10] or 'superomniphobic'[7] was used to describe the nature of these surfaces—both superhydrophobic and superoleophobic.

This tutorial review summarizes the research in this field, describes the analytical methods for superamphiphobicity (section 2), different techniques towards the fabrication of superamphiphobic surfaces by combining design of surface roughness and surface chemistry (section 3), and a variety of existing functional applications (section 4). Finally, a brief overview of the current state and future opportunities in this field is presented.

2. Characterization of superamphiphobicity

A sessile drop will normally form in shape of a sphere sectioned by the surface when it is placed onto a flat substrate. There is a discrete and measurable θ_{CA} between the sphere and the surface at the circular solid/liquid/vapour three-phase contact line. Generally, the surface is regarded as hydrophilic when $\theta_{CA} < 90°$; in other words, the surface is hydrophobic if $\theta_{CA} > 90°$. Specifically, the surface with $\theta_{CA} > 150°$, in addition with a sliding angle $\theta_{SA} < 10°$, is usually named as a super-antiwetting (or super-repellent) surface: the surface is deemed as superhydrophobic if the surface displays only water super-repellency; whereas the surface is acknowledged as superamphiphobic if it exhibits super-repellency towards probing

liquids not only water but also low-surface-tension 'oils'.

The characterization of superamphiphobicity is one of the key issues in the research of superamphiphobic surfaces. The simplest method to characterize a super-repellent surface is eye visualization, in which a gentle flow of a probing liquid is applied to the surface, and the wetting and flowing behaviours are visualized. The surface can be roughly deemed as super-antiwetting if both water and 'oils' can move freely on the surface without any sticking. However, to characterize a super-antiwetting surface quantitatively, precise determinations of static θ_{CA} and CAH, which are normally performed with commercial instruments, are needed.

2.1. Static contact angle

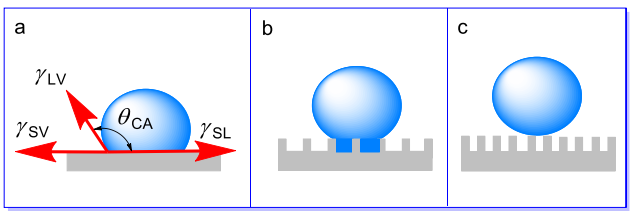

Fig. 2 Schematic illustration of a droplet placed onto a flat substrate (a) and rough substrates (b) and (c). Depending on the roughness of the surface, the droplet is either in the so-called Wenzel regime (b) or the Cassie-Baxter (c) regime.

More than 200 years ago, Thomas Young, the genius polymath who made major contributions to vision, physiology, sound, light, language, solid mechanics, and Egyptology, described the forces acting on a liquid droplet spreading on a surface (Fig. 2a). The θ_{CA} of the drop is related to the interfacial energies acting between the solid-liquid (γ_{SL}), solid-vapour (γ_{SV}) and liquid-vapour (γ_{LV}) interfaces following:

$$\cos\theta_{CA} = \frac{\gamma_{SV} - \gamma_{SL}}{\gamma_{LV}} \quad (1)$$

The above equation known as Young's equation is a clear oversimplification of the real situation as it is strictly valid only for surfaces that are chemically homogeneous, atomically smooth, and those that do not change their characteristics due to interactions of the probing liquid with the substrate, and any other outside force.[11] Notably, there is absolutely no such an ideal surface in the real world. Therefore, two different models, the so-called Wenzel regime[12] (Fig. 2b) and Cassie-Baxter regime[13] (Fig. 2c), were developed to explain the wetting behaviour on a rough surface.

In the Wenzel regime (Fig. 2b), the difference of the measured θ_{CA} from the 'true' contact angle of a flat surface (θ_F) was described as follows:

$$\cos\theta_{CA} = R\frac{\gamma_{SV} - \gamma_{SL}}{\gamma_{LV}} \quad (2)$$

where R is the ratio between the actual surface area of the rough surface and the apparent area. In this regime, surface roughness can promote either wettability ($\theta_{CA} < 90°$) or non-wettability ($\theta_{CA} > 90°$), depending on the chemical property of the surface.

Interestingly, if the surface is composed of small protrusions that cannot be filled by the liquid and are thus filled with air (*i.e.*, trapping of air underneath of the liquid droplet), the wetting phenomenon can be described by the so-called Cassie-Baxter regime:

$$\cos\theta_{CA} = -1 + \Phi_S\left(1 + \frac{\gamma_{SV} - \gamma_{SL}}{\gamma_{LV}}\right) \quad (3)$$

where Φ_S is the fraction of the surface that is in contact with the liquid. In such a case, the liquid touches only the top of the surface with very limited contact area. The corresponding θ_{CA} is always much higher than that of a flat surface composed of the same material since the pores are filled with air, which is hydrophobic. Hence, surface topography plays a very profound effect on the wettability.

2.1.1. Contact angle measurement with a sessile drop of water

θ_{CA} measurement is one of the most important methods for the characterization of a superamphiphobic surface. This can be performed on a commercial instrument [for example, Contact Angle System OCA (Stuttgart, Germany), Krüss DSA Series (Hamburg, Germany), Rame-Hart Goniometers (Succasunna, USA), and CAM Goniometers (KSV Instruments Ltd., Helsinki, Finland)] with a charge-coupled device camera that is used for the recording the image of a water droplet on a surface, and analysis software that provide different fitting models such as circle fitting, ellipse fitting, and tangent searching, and Laplace–Young fitting. The calculated θ_{CA} may vary a lot for the same volume water drop (normally 5 to 10 μl) on the same surface when using different fitting models. For example, the maximum θ_{CA} can be obtained under circle fitting, ellipse fitting, and tangent searching models is around 156°; however, maximum value around 180° will be given when Laplace–Young fitting is adopted.[3] This is because the deformation of a water droplet caused by the gravity was calibrated in Laplace–Young fitting; whereas it was not excluded for the other fittings. Therefore, fitting model should be mentioned when reporting data of θ_{CA}.

In our work,[14] we realized that a good optical presentation of the water droplet is crucial to get reproducible θ_{CA}. Besides, the obtained value can also be affected by the focus of the camera, light intensity, contrast of the image, and the settlement of the three phase contact baseline, especially when $\theta_{CA} > 150°$. For example, the apparent value from the same droplet may vary from 165° to 175° by only a small tuning of the above parameters. Therefore, θ_{CA} at various positions are normally recorded so as to get a more trustable average value.

2.1.2. Contact angle measurement with a sessile drop of a low-surface-tension, organic liquid

Sessile drop measurement with water is not sufficient for the characterization of a superamphiphobic surface; in such a case, θ_{CA} test with low-surface-tension liquids should be performed in addition.[9,15] Such probing liquids are mainly non-polar alkanes such as *n*-hexadecane, *n*-dodecane, *n*-decane, and cyclohexane,[9,15,16] but polar solvents such as toluene, diodomethane,[9] and any other oils (*e.g.*, mineral oil and cooking oils) are also frequently used.[9,16] Generally, θ_{CA} of different liquids on the same surface decreases with the increase of the surface tension of the probing liquid (Fig. 3).[16] That's why 'oils' spread quickly on a solely

superhydrophobic surface[15] and θ_{CA} analysis with 'oils' is needed for the characterization of superamphiphobicity.[9,15] As is clearly shown in Fig. 3, flat silicon is both hydrophilic and oleophilic; porous silicon (PS) is superhydrophobic but superoleophilic; *1H,1H,2H,2H*-perfluorooctyl trichlorosilane (PFOTS) coated silicon (FTS-Si) is hydrophobic but oleophilic; PFOTS coated porous silicon (FTS-PS) is both superhydrophobic and superoleophobic, *i.e.*, superamphiphobic.

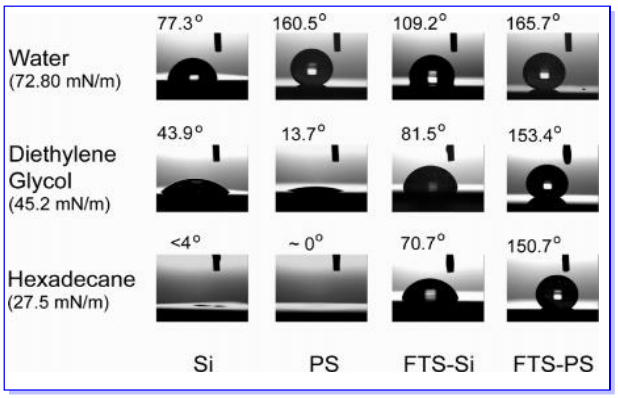

Fig. 3 Static contact angles of water, diethylene glycol, and hexadecane on flat silicon (Si), porous silicon (PS) with tilted pores, flat silicon coated with FTS (FTS-Si), and porous silicon with tilted pores coated with FTS (FTS-PS). Reprinted with permission from ref. 16, ACS copyright 2008.

2.2. Contact angle hysteresis

Whether surfaces displaying $\theta_{CA} > 150°$ for probing liquids both water and 'oils' are truly superamphiphobic remains unknown if the corresponding CAH is not determined. For example, despite a high θ_{CA} (*ca.* 160°) for rapeseed oil on a superhydrophobic surface composed of surface-fluorinated carbon nanotubes, the oil droplet remained pinned of the surface when the substrate was tilted.[17]

Any real surface exhibits two contact angles, the so-called advancing contact angle (θ_{Adv}) and receding contact angle (θ_{Rec}). The difference between them is a presentation of the surface 'non-ideality', and commonly referred to as the CAH,[11] which is intimately related to the adhesion of materials on the surface. Conventionally, superhydrophobicity means not only a high θ_{CA} but also a low CAH because the low hysteresis is responsible for the self-cleaning behaviour.[3] Therefore, CAH measurement is the other most important method for the characterization of a superamphiphobic surface. Many techniques have been developed up to date to characterize the CAH, and amongst of them $\theta_{Adv}/\theta_{Rec}$ and the tilt angle are the most often used ones.

2.2.1. Advancing/receding contact angle

$\theta_{Adv}/\theta_{Rec}$ can be measured by a commercial instrument with an enhanced video microscopy system incorporating digital image analysis, for example, Krüss DSA (Germany). A syringe pump is used to generate a water droplet on the substrate, and to control the rate of water pumping and suction through the needle to perform the advancing and receding, respectively. After the drop-forming step, water is continuously and slowly pumped into (or sucked from) the droplet at a rate smaller than 0.3 ml·min^{-1} and θ_{Adv} was recorded simultaneously by a frame grabber *via* a solid state charge coupled device camera (Fig. 4a, right). In the last step, the water droplet is receded and θ_{Rec} is recorded (Fig. 4a, left).[18]

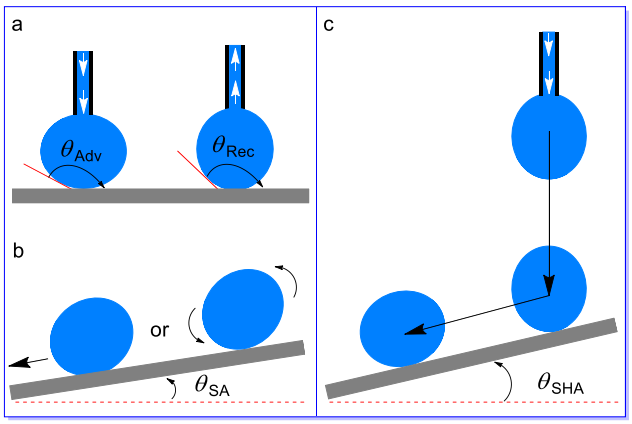

Fig. 4 Schematic illustration of the techniques for the determination of contact angle hysteresis: advancing θ_{Adv} and receding contact angle θ_{Rec} (a); tilt angle, *i.e.,* the so-called roll off angle or sliding angle θ_{SA} (b); and shedding angle θ_{SHA} (c).

2.2.2. Tilt angle

The tilt angle refers to the critical angle between the substrate and the horizontal, below which the droplet starts to move upon elevating one end of the substrate. It should be pointed out that the tilt angle reflects, but not equals to, the difference between θ_{Adv} and θ_{Rec}.[3] A low tilt angle is crucial to the so-called self-cleaning behaviour, and superamphiphobic surfaces should show a tilt angle lower than 10° for both water and 'oils'. The tilt angle measurements have two types—the sliding angle θ_{SA} (Fig. 4b) for macroscopically flat surfaces and the shedding angle θ_{SHA} (Fig. 4c) for macroscopically rough surfaces.

The sliding angle, also known as the roll-off angle, indicates the angle of inclination of a surface when a droplet completely rolls off of the surface due solely to gravity. In experiments, the θ_{CA} measuring instrument is equipped with an additional accessory—a tilt plate with tunable angle between 0° and 90°. The tilt angle is increased continuously from 0° to 90°, and the angle is recorded as θ_{SA} while the droplet is sliding away or rolling off the surface.[9,15,19] Strictly speaking, there is a slight difference between sliding and rolling since the way of droplet moving on the tilt surface is not the same (Fig. 4b). In the former case, the surface area of the droplet contacting with the substrate is slightly higher and fixed because of the high adhesion force in between. In contrast, for the latter case, the contacting area and the adhesion in between are slightly lower, and thereby the droplet rolls freely on the surface. Nevertheless, in most cases they are treated equally since the only important thing is the tilt angle where the droplet moves away rather than the moving manner. The only exception is the case of slippery liquid surfaces—liquids on such surfaces slides freely but unable to roll due to their special surface structure and unique surface chemical component.[20–22]

θ_{SA} becomes impractical when macroscopically rough substrates such as cotton fabrics and wools are measured.[19] In order to characterize the superhydrophobicity of a

macroscopically textile, a new technique named shedding angle was developed recently.[14] In essence, a water drop of defined volume is released onto the substrate from a defined height. The minimum angle of inclination at which the substrate needs to be tilted for the drop to completely roll or bounce off the substrate is determined (Fig. 4c). Four parameters were controlled: the tilt of the substrate, the needle-to-substrate distance, the relative distance of the impact point to the lower end of the substrate, and the drop volume. More details about the measuring procedure can be seen in ref. 14.

3. Fabrication techniques towards superamphiphobicity

In this section, the fabrication techniques towards superamphiphobic surface will be described and discussed. As is well-known, the combination of appropriate surface roughness and surface chemistry is crucial to the preparation of superhydrophobic surfaces. Therefore, two steps, *i.e.*, the generation of nanoscale roughness and the functionalization with low surface energy materials (mainly fluorinated small molecules or macromolecules), are involved. Depending on the sequence of the above two steps in the preparation process of a superamphiphobic surface, the fabrication strategies can be classified as the following three strategies (Fig. 5): (1) the 'pre-roughening + post-fluorinating' technique (section 3.1); (2) the 'pre-fluorinating + post-roughening' technique (section 3.2); and (3) the generating of surface roughness and surface fluorinating occurs in the same step, *i.e.*, one-pot or *in situ* fabricating techniques (section 3.3). It should be pointed out that some of the so-called superamphiphobic surfaces that are not truly superamphiphobic (because of their relatively high CAH) are included in this section.

3.1. 'Pre-roughening + post-fluorinating'

The pre-roughening and post-fluorinating methods appeared up to date will be separately discussed in this section because each of them contains a variety of different ways and there are a lot of combinations that may overlap with each other.

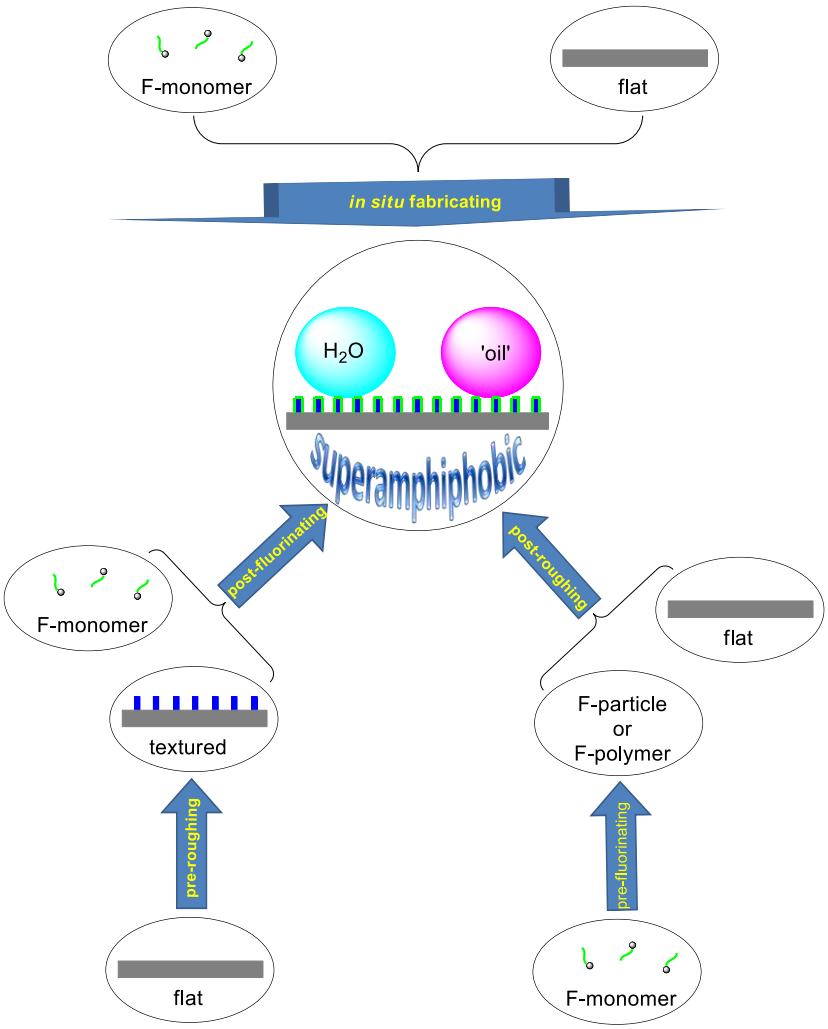

Fig. 5 Three strategies towards the fabrication of superamphiphobic surfaces: pre-roughening + post-fluorinating (section 3.1); pre-fluorinating + post-roughening (section 3.2); one-pot *in situ* fabricating (section 3.3).

3.1.1. Pre-roughening a substrate

3.1.1.1. Functionalization with nanoparticles (NP)

Functionalization with nanopartciles represents an important method to generate nanoscale roughness on a substrate. The nanoparticles can be nanosilicas, silicone nanofilaments, carbon

nanotubes, carbon nanofibers, and so on.

Nanosilica is a common type of nanomaterials that are inexpensive and frequently used in the fabrication of surface roughness.[23–25] For example, Leng *et al.*[23] functionalized woven fibers with a layer of microscale silica *via in situ* Stöber reaction, followed by further modification with another layer of nanoscale silica *via* physical adsorption. Briefly, a piece of cotton textile was immersed in a room temperature mixture of methanol, isopropanol, and ammonium solution in the presence of tetraethylorthosilicate for several hours, and then cleaned with methanol in an ultrasonic bath repeatedly so as to remove the physically adsorbed particles. Subsequently, the obtained textile was soaked in 3-aminopropyltriethoxysiloxane solution to generate surface amine groups which were then protonated with hydrochloric acid. The positively charged textile was then dipped into a suspension of negatively charged nanosilicas, resulting in a layer of silica nanoparticles because of electrostatic attraction. On the contrary, Hsieh and coworkers[24] applied hierarchical silica sphere stacking layers to glass surface *via* self-assembly technique. It involves a two-stage spin coating of two different silica spheres with diameter of 20 nm and 300 nm, respectively. A gravitational sedimentation for 2 days made the silica spheres fall onto the surface of the substrate, thus forming a well-organized sphere arrays—a closed hexagonal arrangement. A number of large spheres were firstly stacked, followed by the secondary stacking of small silica spheres. He *et al.*[25] spun–coated a mixture of polydimethylsiloxane (PDMS) and nanosilica onto glass substrates, followed by stintered at 500 °C for 2 h. And the obtained coatings showed higher stability than those just fabricated by spin-coating nanosilica.

For carbon nanotubes (CNTs), numerous applications have been found in many areas of science and engineering because of their excellent electronic, mechanical, and chemical properties. Recently, they were used to create surface roughness so as to impart super-repellent properties to the resultant surfaces.[26,27] For example, Zhang and coworkers[27] demonstrated that superamphiphobic surface could be obtained perfluorosilane-rendered TiO_2/single-walled carbon nanotube composite coatings. Interestingly, the wetting ability of such coatings could be tuned from superoleophobic to superoleophilic *via* ultraviolet irradiation. Moreover, by controlling the dose of UV illumination, superphobicity and superphilicity can exist on the same surface for probing liquids with different surface tensions. Except nanosilica and carbon nanotubes, carbon nanoparticles such as carbon nanofibers,[28] fullerene, graphene as well as other inorganic particles such as nano ZnO_2, CuO, $Ca(OH)_2$ and $CaCO_3$ has also been reported to generate surface roughness (see the related references in ref. 25).

Coating a substrate with polyalkylsilsesquioxane filaments (named as silicone nanofilaments, SNF), first reported in 2004, represents an economical and efficient way to prepare super-repellent surface.[29] With this technique,[9,14,15,19,29,30] a dense SNF layer can be grown on various substrates, including glass, silicon, ceramics, Titanium, Aluminium, cotton fabrics, silk, wood, polyethylene, and so on, by either gas[19,30] or liquid (wet toluene)[9] phase deposition of trichloromethylsilane (TCMS) in the presence of a trace amount of water (*ca.* 50 ppm to 200 ppm)[9] at room temperature (Fig. 6). The as-prepared surface shows extremely water-repellent properties since SNF imparts the surface with not only nanoscale roughness but also low-surface-energy. Besides, such a coating exhibits excellent chemical[31] and environmental stability.[32]

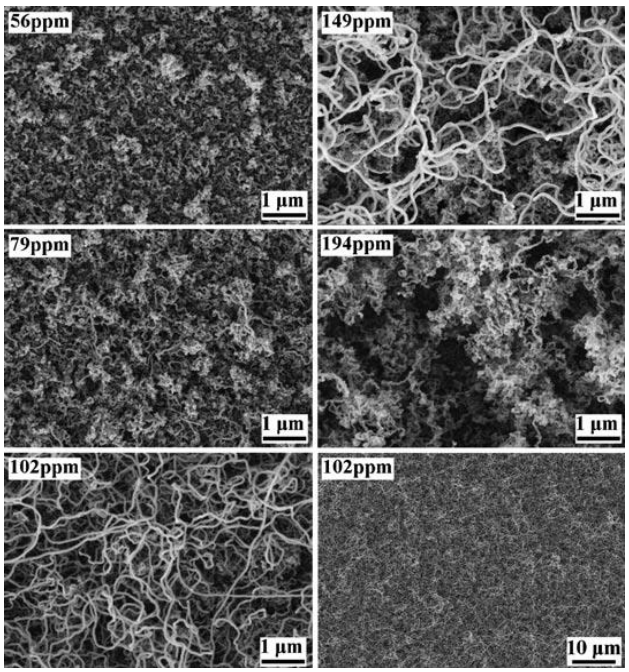

Fig. 6 Surface morphology of the TCMS-coated glass slides at different water concentrations in toluene during the TCMS coating procedure. Scale bars: 1 mm, except for the image at the bottom right corner (10 mm). Reprinted with permission from ref. 9, copyright Wiley 2011.

3.1.1.2. Etching

Etching[33–41] is a facile and inexpensive method that is frequently used in creating surface roughness. Depending on the nature of the substrate, etching techniques can be classified into the following types: acid etching,[33] base etching,[34,35] electrochemical etching,[36] Au-assisted electro-chemical etching,[37] ion etching,[39] plasma etching,[40] and others[41].

Using engineering metal such as aluminium and its alloys as substrates, Yang *et al.*[33] developed a simple method to achieve hierarchical textured surface morphology by HCl etching and boiling water treatment. Differently, copper substrate can be etched by a base-assist surface oxidation process,[34,35] leaving the surface with hierarchical structure composed of CuO microflowers and $Cu(OH)_2$ nanorod arrays.[34] Briefly, copper sheets were immersed in a NaOH solution in the presence of $NH_4S_2O_8$ at room temperature.[34] However, Titanium cannot be etched by either acid or base, but can be etched by electro-chemical methods. For example, micro-textured Ti can be obtained by electrochemically etching a titanium foil in a dilute NaCl solution at a constant voltage of 15 V for 1 h, as reported by Kim *et al.*[36] Upon further immersing the micro-patterned Ti into a concentrated NaOH solution at 120 °C for 3 h, and subsequently cleaned by dilute HNO_3 and deionized water, TiO_2 nanotube arrays on top of the micro-textured Ti was obtained.

P-type (100) silicon can be roughened *via* an electrochemical etching process. As reported by Cao *et al.*,[37] p-type Si (100) with vertically aligned straight pores was fabricated by anodic etching of Si (100) chips in a Teflon electrochemical cell in the presence

of a solution of HF/ethanol and a direct current at a density of 100 mA/cm^2. In contrast, p-type Si (111) film with tilted pores was fabricated using a gold-assisted electroless etching process.[37] In such a case, the Si (111) film was first coated with Au nanoclusters by dipping in a $KAuCl_4$/HF solution; and then it was etched in a $Fe(NO_3)_3$/HF solution at 50 °C, during which the Au nanoclusters served as an electrochemical reaction center. Differently, n-type Si (100) film with surface pyramid structure can be prepared by etching the substrate in a aqueous solution of KOH and isopropanol at 85 °C for 20–30 min.[38] Glass can be tailored by ion etching, and subsequently chemical etching in aqueous HF.[39]

Besides the etching techniques discussed above, other etching methods such as plasma etching[40] and water etching[41] can also be applied, depending on the chemical property of the substrate.

3.1.1.3. Lithography

Lithography is a useful method for fabricating rough surfaces with regular structures. For example, well-defined structures, including pillars with wavy side walls (Fig. 7a),[42] straight smooth side walls (Fig. 7b),[42] and overhang re-entrant structures (Fig. 7c)[42] as well as grooved textures (Fig. 7d)[43] were fabricated by Zhao and coworkers *via* roughening a silicon wafer with a conventional photolithographic technique using a mask, transferring the pattern of mask to the wafers.[42,43] Similarly, on a large-size template of the transparent PDMS elastomer surface, perfectly ordered microstructures with an inverse-trapezoidal cross section (Fig. 7e) were fabricated by Im *et al.*[44] *via* two consecutive PDMS replication processes and a three-dimensional diffuser lithography technique.

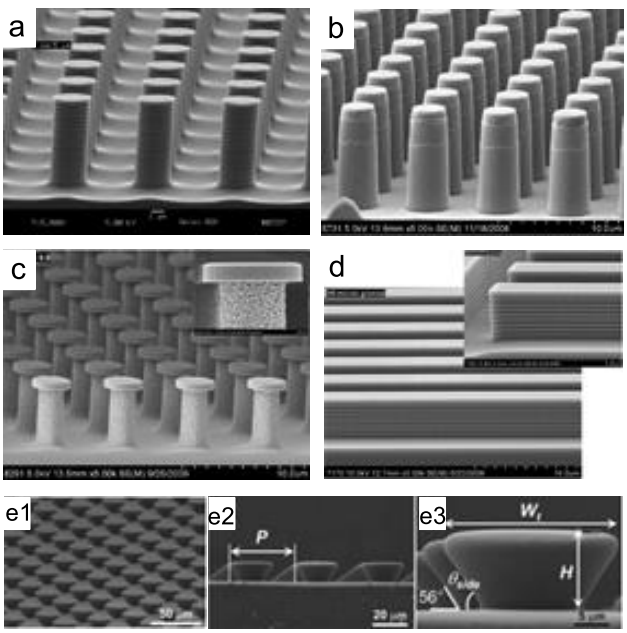

Fig. 7 Well-defined structures prepared *via* Lithography. Figs. 7a, 7b, and 7c were reprinted with permission from ref. 42, ACS Copyright 2011; Fig. 7d was reprinted with permission from ref. 43, ACS Copyright 2012; Fig. 7e was reprinted with permission from ref. 44.

In a recent work reported by Susarrey-Arce and coworkers,[45] arrays of microstructures were successfully fabricated by reactive ion etching of a silicon wafer, which was covered by a patterned photoresist layer. By using the same pitch of a photolithographic mask, the influence of SF_6, O_2 and CHF_3 gases during the etching process was investigated. Further, it was demonstrated that homogeneous pedestal-like structures can be fabricated by varying the loading conditions during the etching process. The roughness of the microstructures could also be tuned by changing the dry plasma etching conditions.

3.1.1.4. Template-assisted synthesis

Template assisted synthesis is also frequently employed in fabricating surface roughness.[3]

Deng and coworkers[46] reported a template-assisted synthesis of nanosilica by using candle soot as a template. The deposition of a soot layer was completed by simply exposure a glass slide to the flame of a paraffin candle, which turned the glass black. SEM revealed that the soot consists of a fractal-like network composed of carbon particles with diameters between 30 nm and 40 nm. However, the structure is fragile because the particle-particle interactions are only physical and are weak. When water rolls off the surface, the drop carries soot particles with it, and finally all of the soot deposit can be removed. Inspired by the promising morphology of soot, the authors developed a technique to coat the soot layer with a silica shell, making use of chemical vapor deposition (CVD) of tetraethoxysilane (TES) catalyzed by ammonia. Similar to a Stöber reaction, silica is formed by hydrolysis and condensation of TES. The shell thickness can be tuned by the duration of the CVD process. For example, after 24 h coating, the carbon particles were covered by a 20 nm–thick silica shell. Calcinating the hybrid carbon/silica network at 600 °C for 2 h in air resulted in the combustion of the carbon core and the decrease in the shell thickness, but the surface roughness and network texture could be retained.

In Ganesh *et al.*'s work,[47] a one-dimensional morphology of nanofibers was used as a template to prepare a robust and transparent superamphiphobic coating. The template was fabricated by the deposition of a thick layer of SiO_2 nanofibers on glass. The developed template was subsequently coated with a 25 nm porous silica membrane by vapour phase deposition of triethoxysilane. After 600 °C heat treatment, a transparent, superhydrophilic coating consisting of a hybrid silica network (branched SiO_2 nanofibers with surrounding silica membrane) was obtained. It was observed that during the annealing, the coated silica membrane reinforced the SiO_2 nanofibers and prevented the fibers from disintegrating into nanoparticles, generating a hybrid silica network. The fiber morphology plays an important role in assisting the hybrid silica network to keep its roughness and surface texture.

3.1.1.5. Sputter deposition

Sputter deposition stands for another useful method that can be used for the fabrication of surface roughness. For instance, Fujii *et al.*[48] prepared hierarchical submicrometer-nanometer dual pillar surfaces with optimized pillar intervals *via* sputtering Al-Nb alloys onto aluminium substrates, followed by further anodizing. In a subsequent work,[49] the authors replaced the Al-Nb with Al, and as a result Al was sputter deposited. Nanopores were developed through an anodizing process, forming a nanoporous anodic aluminium layer.

3.1.1.6. Galvanic replacement reaction

Galvanic replacement reaction is a single step reaction that utilizes the differences in the standard electrode potentials of various metal elements, leading to the deposition of the more noble metal element and the dissolution of less noble metal element. For example, roughened hierarchical micro/nanostructured Ag deposited layers on Zn substrates were developed *via* galvanic replacement reactions by Zhang and coworkers.[50] Briefly, Zn plates, either those without any pre-treatment or those treated for 2 h in a –20 °C refrigerator or in a 80 °C oven, could be used as the substrates. The galvanic replacement reactions were carried out by simply immersing the substrates in aqueous $AgNO_3$ for various time intervals, followed by cleaning with deionized water and drying in air. The surface morphology and roughness can be altered through the tuning of the solution concentration, the immersing time, and the pre-treating temperatures.

3.1.1.7. Sol/gel synthesis

Sol/gel transition represents another useful technique that can be employed in fabricating surface roughness.[51,52] For example, superoleophobic nanocellulose aerogels have been prepared using unmodified cellulose nanogels, which normally have surface structure with robust network at several length scales because of the presence of the individual nanofibers as well as their self-assembly aggregates.[51] These gels are usually prepared following a sol/gel transition process. A typical procedure is as follows: a pulp suspension was diluted to 3% consistency firstly, and then the cellulose nanofibers were disintegrated using an ultrafine friction grinder, which consists of a lower and an upper stationary SiC grinding stone with a gap of 100 μm. Water was added during the grinding process, inducing the formation of a nanocellulose hydrogel. Using silica aerogel as a model material, Jin and coworkers[52] prepared superamphiphobic silica aerogel by vapour phase deposition of a fluorinated monomer. Such a surface displays excellent mechanical stability because of its self-similar network structure, which allows fresh re-entrant surface topography even after the removal of the uppermost layer upon mechanical abrasion.

3.1.2. Post-fluorination of a pre-roughened surface

After surface roughness is created, the substrates must be further chemically modified with low-surface-energy materials, normally fluorinated compounds, so as to achieve superamphiphobicity. Generally, a fluorinated layer can normally be produced by depositing molecular perfluoroalkane with a functional group at one terminal (F-monomer, Fig. 8), for instance, *1H,1H,2H,2H*-perfluorooctyl phosphate (PFOP),[48,49] *1H,1H,2H,2H*-perfluorooctanoic acid (PFOA),[33,34] *1H,1H,2H,2H*-perfluorooctyl trichlorosilane (PFOTS),[15,36–40,42–47,51] *1H,1H,2H,2H*-perfluorodecyl trichlorosilane (PFDTS),[9,27,41] *1H,1H,2H,2H*-perfluorodecane-1-thiol (PFDSH),[35,50] *1H,1H,2H,2H*-perfluorodecyl acrylate (PFDAE).[53] However, it can also be achieved by spin-coating a fluorinated-polymer (F-polymer) solution. While grafting a fluorinated layer by using F-monomers, the process can be carried out *via* either vapour[39,42–47,51] or liquid[33–38,40,41,48–50] phase deposition.

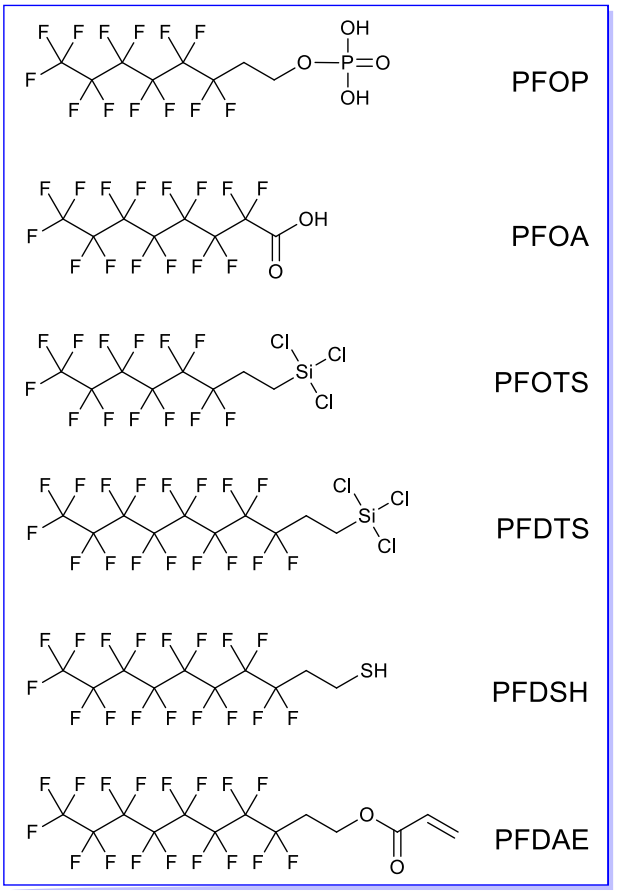

Fig. 8 Chemical structures of functionalized-perfluoroalkanes used in the surface modification of a roughened substrate.

3.2. 'Pre-fluorinating + post-roughening'

Different from the methods discussed in section 3.1, "pre-fluorinating + post-roughening" represents another strategy to fabricate superamphiphobic surface. In such a case, fluorinated polymers or nanoparticles were synthesized firstly, and subsequently applied to flat surfaces *via* spin-coating, spray-coating, dip-coating, electrospinning, sol/gel transition, or other physical techniques, generating roughened structures with a low-surface-energy layer on the surface. This section is organized according to the different techniques and chemical components that are frequently used for the surface modification of a flat surface.

3.2.1. Spinning or spraying fluorinated silica nanoparticles

Sheen *et al.*[54] reported a method to prepare fluorinated silica nanoparticles (FSN). Briefly, ammonium hydroxide was added to a mixture of tetraethoxysilane (TEOS) and isopropanol, and the reaction mixture was refluxed at 60 °C so as to induce of the growth of silica nanoparticles *via* sol-gel transition. Finally, PFDTS was introduced to terminate the reaction until the sol/gel process was running for 100 min, leaving the silica nanoparticles with an outer fluorinated layer. The substrates (glass slides) after being spun-coated using these fluorinated silica nanoparticles become superamphiphobic with θ_{CA} higher than *ca.* 150° for both water and a variety of 'oils'.

Similarly, Campos and coworkers[55] prepared FSN by

fluoroalkyl-functionalizing commercial nanosilicas also using PFDTS. These functionalized nanosilicas were dispersed in a mixture of 5 mg/ml commercial fluoropolymer Viton ETP-600S (DuPont) in 1,3-dichloro-1,2,2,3,3-pentafluoropropane, forming a suspension with silica concentration ranging from 0% to 80% (w/w). The fresh FSN suspension was spray-coated onto silicon wafers through an airbrush with a 1.06 mm diameter tip using compressed air, which was repeatedly passed over the substrates laterally at a distance of *ca.* 15–20 cm. Finally, the samples were air-dried for 1h, followed by further drying at 60 °C for 12 hours. The as-prepared surfaces showed superhydrophobicity when FFNS concentration is higher than 20% (w/w). To achieve superoleophobicity for probing liquid of CH_2I_2 and rapeseed oil, FFNS concentration of 40% and 70% are needed, respectively. While FFNS concentration equals to 80%, the surface exhibited θ_{CA} about 160° for hexadecane; however, the corresponding θ_{SA} is much higher than 20° due to the extremely low surface tension of hexadecane (γ_{LV} = 27.5 mN·m^{-1}).

3.2.2. Spraying fluorinated carbon nanotubes

Wang and coworkers[56] synthesized fluorinated multi-wall carbon nanotubes (MWCNTs-PFOL) by grafting *1H,1H,2H,2H*-perfluorodecanol (PFOL) onto multi-wall carbon nanotubes (MWCNTs). Then a nanocomposite containing polyurethane pre-polymers, PFOL, hexanediol, a mixture of acetone and toluene and MWCNTs-PFOL was spray-casted onto glass slide. The obtained coating shows coralline-like structure (Fig. 9a) and displays θ_{CA} greater than 150° for probing liquids not only water but also 'oils' (Fig. 9b). The CAH is low for water (θ_{SA} = 5°) but slightly higher for low-surface-tension oils such surfactant solution (θ_{SA} = 15°), glycerol (θ_{SA} = 10°), CH_2I_2 (θ_{SA} = 30°), rapeseed oil (θ_{SA} = 35°), and hexadecane (θ_{SA} = 40°).

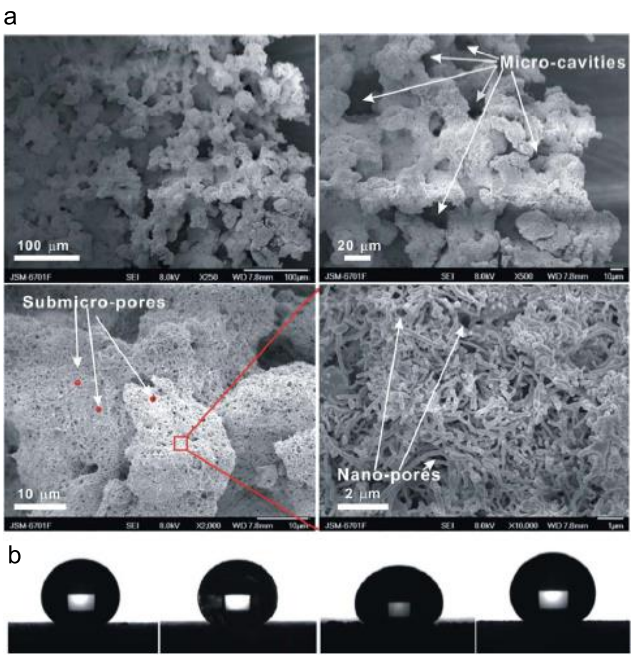

Fig. 9 SEM images of the surface morphology of perfluoroalkyl grafted MWCNTs/PU nanocomposite coatings at different magnifications (a): multiscale structure with numerous micro-cavities, micro- and nano-pores are formed; and profile images of liquids: water, glycerol, CH_2I_2, and hexadecane from left to right (b). Reprinted with permission from ref. 56.

3.2.3. Spraying a copper perfluorooctanoate suspension

Yang *et al.*[57] reported a simple method to prepare copper perfluorooctanoate by reacting copper acetate with perfluorooctanoic acid in aqueous media. Uniform coatings with robust superoleophobicity were produced by spraying the copper perfluorooctanoate suspension onto various substrates. Such coatings displayed apparent θ_{CA} greater than 150° and low sliding angles, even with liquids possessing a significantly lower surface tension, such as hexadecane and dodecane. The robust superoleophobicity was ascribed to the re-entrant morphology and extremely low surface energy, which can effectively prevent the transition from the Cassie–Baxter state to the Wenzel state. Such a facile technique shows great potential for a wide range of applications because it can be applied to a variety of substrates without limitations of size and shape, do not typically require complicated application methods and can be easily repaired after being mechanically damaged.

3.2.4. Electrospinning or spraying a blend of a fluoroalkyl polyhedral oligomeric silsesquioxane and a common polymer

Electrospinning is a versatile technique for producing micro/nanofibers from a variety of polymers.[58] In a laboratory environment, it requires a high-power supply, a syringe pump, a conducting substrate, and a polymer with high molecular weight as a starting material. The electrospinning process is initiated by a high electric field between the syringe that containing viscous polymer solution and the conducting substrate. A charged liquid jet is ejected from the tip of a distorted droplet because of the high electrical potential. The liquid jet experiences whipping and bending instabilities within a sufficient distance to evaporate its solvent thoroughly and, consequently, becomes a solid micro/nanofiber membrane on the substrate. Recently, superamphiphobic surfaces have been fabricated by electrospinning a blend of a fluorinated polymer and a common polymer.[5,7]

Tuteja and coworkers[5] synthesized a class of hydrophobic polyhedral oligomeric silsesquioxane (POSS) molecules in which the rigid silsesquioxane cage is surrounded by *1H,1H,2H,2H*-perfluorodecyl or *1H,1H,2H,2H*-perfluorooctyl groups (referred to as FD-POSS and FO-POSS, respectively). The high surface concentration and surface mobility of $–CF_2–$ and $–CF_3$ group, along with the high ratio of $–CF_3/–CF_2–$, results in a strongly hydrophobic material with low-surface-energy. A spin-coated film on a flat Si wafer, which had a root mean square roughness 3.5 nm, exhibited θ_{Adv} and θ_{Rec} about 124.5 ± 1.2° for probing liquid of water. Surprisingly, rough structure composed of beads-on-strings fibers displaying superhydrophobicity and extremely oleophobicity (but not superoleophobicity) was prepared by electrospinning a 5% (w/w) blend of FD-POSS/poly(methyl-methacrylate) (PMMA) when FD-POSS mass fraction is higher than ~0.1, though the corresponding spin-coated surfaces are oleophilic. It was demonstrated that the local surface curvature plays a key role in driving the oleophobicity, and the electrospinning coating technique can also be applied to fragile or natural substrates so as to confer oleophobicity in addition to superhydrophobicity. In a subsequent work,[7] the authors extended their work by developing four dimensionless design parameters that describe the robustness of a composite interface and the

observed apparent θ_{CA} on a textured surface, given the various thermophysical and geometric properties that parameterize the system. Guided by the design parameters, they developed families of superamphiphobic surfaces by systematically varying the various chemical and topological surface features. Beads-only, beads-on-strings, and fiber-only structures are formed at a solute concentration of 2%, 5%, and 10% (w/w), respectively. Interestingly, θ_{Adv}, θ_{Rec}, and θ_{SA} for hexadecane on the beads-only surface are 156°, 150° and 5°, respectively. In comparison, the beads-on-strings and fibers-only surfaces shows a slightly higher CAH with $\theta_{Adv}/\theta_{Rec}$ values of 153°/141° and 153°/134°, respectively. Recently, the same research group demonstrated that similar textured surfaces can also be fabricated by spraying the FD-POSS/PMMA blend.[59] Very recently, Pan *et al.*[60] employed an electrospun coating of cross-linked poly(dimethylsiloxane) + 50% FD-POSS (w/w) on top of stainless steel wire meshes to fabricate hierarchically structured surfaces. Such a surface possesses re-entrant curvature at both the coarser length scale and the finer length scale. The hierarchical texture along with the re-entrant curvature and the low surface energy of the coating resulted in a superamphiphobic surface with extremely high θ_{CA} and low CAH for a range of different polar and nonpolar low surface tension Newtonian liquids, including various acids, bases, and solvents.

Opposite to the procedures discussed above,[5,7,59,60] by dissolving FD-POSS in a low-molecular-weight fluorinated compound, *1H,1H,2H,2H*-perfluorobutyl triethoxysilane, Lin *et al.*[61] prepared a viscous solution, which was then dispersed in ethanol. Upon ultrasonication for 0.5 h, a stable, homogeneous suspension was obtained. Such a dispersion can be easily applied onto fabrics so as to impart superamphiphobicity to the surface through a wet-chemical coating technique such as spraying, dip-coating, or padding.

3.2.5. Coaxial electrospinning a fluorinated polymer and a common polymer

In contrast with electrospinning, coaxial electrospinning expands the versatility of electrospinning by enabling the formation of core-sheath-structured micro/nanofibers. A coaxial nozzle consists of a central tube surrounded by a concentric annular tube. As reported by Steckl *et al.*,[58] a fluoropolymer Teflon AF2400 solution and a common polymer poly ($\mathcal{E}$-caprolactone) was used as sheath and core material, respectively. Both solutions were separately fed into the coaxial nozzle from which they were ejected simultaneously. A compound pendant droplet was generated from the coaxial nozzle without bias; upon application of a sufficient voltage, a Taylor cone was formed and a liquid jet was ejected that consists of the core material enveloped by the sheath material. Then the polymer jet underwent the same process as in conventional electrospinning: being pulled by the electric field and whipped and stretched by the bending instability, followed by evaporation of the solvent causing the formation of solid-state fibers. Coaxial electrospinning technique allows the resulted fibers combine different characteristics from both the core and the sheath polymers.

3.2.6. Sol/gel transition of a fluoropolymer

In the work by Xiong *et al.*,[62] a diblock copolymer, poly[3-(triisopropyloxysilyl)propylmethacrylate]-block-poly[2-(perfluorooctyl)ethyl methacrylate], which contains a fluorinated block and a sol/gel forming block, was synthesized by sequential anionic polymerization firstly. And then the diblock copolymer was chemically grafted onto silica particles by inducing sol/gel transition of the poly[3-(triisopropyloxysilyl)propylmethacrylate] block using α,α,α-trifluorotoluene/tetrahydrofuran mixture as a solvent and HCl as a catalyst, generating a polymer monolayer on the surface of silica particles at sufficiently high P1-to-silica mass feed ratios. Finally, the polymer-silica composite was cast-coated onto glass slides and printing paper, leaving the substrate surface with rugged polymer/silica films, which were superamphiphobic.

3.3. One-pot methods

Compared with the two strategies discussed above, *in situ* synthesis stands for a simpler way to fabricate superamphiphobic surface, and thus was also frequently reported.

Jiang's group[63] developed a one-step electrodeposition process for the fabrication of superhydrophobic surfaces on a series of electrically conductive substrates such as copper, titanium, iron, zinc, aluminium, and tin, using *n*-tetradecanoic acid as an electrolyte. Hierarchical micro/nanostructures with excellent superhydrophobicity were obtained. Such coatings showed superhydrophobicity even for some corrosive liquids including salt solutions and acidic and basic solutions at all *p*H values. By replacing *n*-tetradecanoic acid with nonadecafluorodecanoic acid,[63,64] the authors were able to prepare superamphiphobic coatings with microcluster of flowerlike structures composed of nanosheets. The superamphiphobicity of the treated surface was attributed to synergistic effect of their special surface compositions and textured structures. Compared with traditional approaches towards the preparation of superamphiphobic coatings, this one-pot method is much simpler and the procedure is more convenient to operate.

In Lin and coworkers' work,[65] electrically conductive superamphiphobic coatings were prepared *in situ* by one-step vapour-phase polymerisation of polypyrrole in the presence of a fluorinated alkyl silane on fibrous substrates. In a subsequent work,[66] a robust, electrically conductive, superamphiphobic fabric was prepared by vapour-phase polymerisation of 3,4-ethylenedioxythiophene on fabric in the presence of FD-POSS and *1H,1H,2H,2H*-perfluorooctyl triethoxysilane (FAS). The incorporation of FD-POSS and FAS into the polymeric layer improved the washing and abrasion stability considerably but had a very small influence on the conductivity. The coated fabric can withstand no less than 500 cycles of standard laundry and 10 000 cycles of abrasion test without apparently changing its superamphiphobicity, though the conductivity showed a small reduction. Besides, the coating exhibited self-healing property, *i.e.*, it auto-repair its surface from chemical damages so as to restore its superamphiphobicity.

Saraf and coworkers[67] developed three different techniques to achieve superamphiphobicity using hydroentangled nylon nonwoven fabrics as substrates: (1) pulsed plasma polymerization of *1H,1H,2H,2H*-perfluorodecyl acrylate; (2) microwave-assisted condensation of *1H,1H,2H,2H*-perfluorodecyltrimethoxysilane (FS); (3) FS condensation through wet processing. The coated nonwoven fabrics showed very high θ_{CA} for both water (θ_{CA} = 168–174°) and dodecane (θ_{CA} = 153–160°).

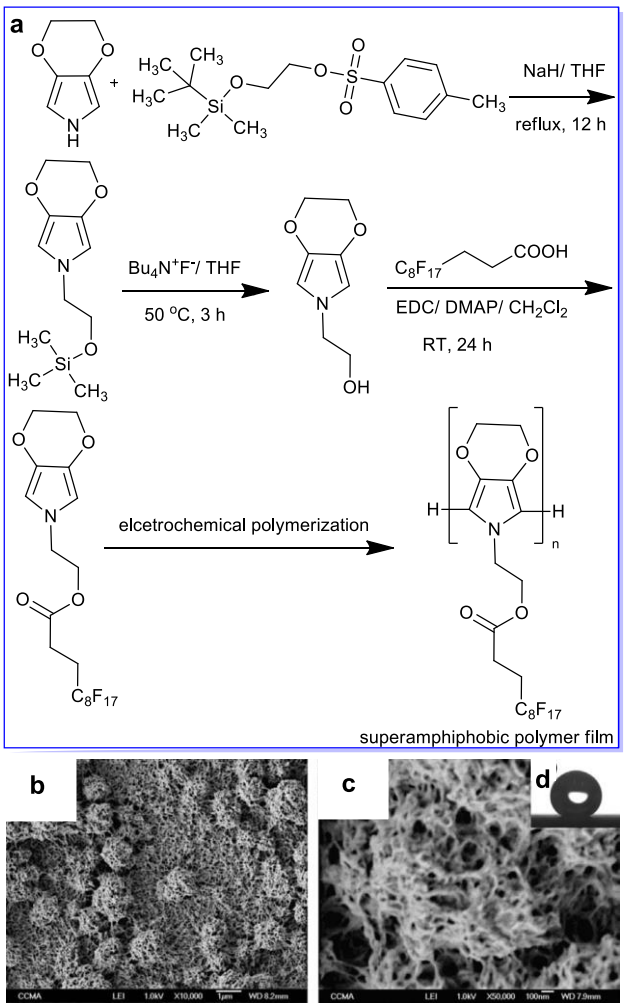

Fig. 10 Synthesis (a) and SEM images (b and c) of the polymeric surface, and a photo of a hexadecane droplet on the surface (d). The scale bar represents 1 μm (b) and 100 nm (b), respectively. Reproduced with permission from ref. 68, copyright 2009 by Academic Press.

Darmanin and Guittard[68] prepared superamphiphobic nanoporous films by electrochemical polymerizing a fluorinated monomer 2-(2,3-Dihydro-[1,4]dioxino[2,3-c]pyrrol-6-yl)ethyl *1H*,*1H*,*2H*,*2H*-perfluorodecanoate, which was synthesized from 3,4-ethylenedioxypyrrole *via* a multi-step procedure (Fig. 10a). The electrochemical polymerization of the monomer was carried out by cyclic voltammetry using a solution of mixture of monomer/tetrabutylammonium hexafluorophosphate in anhydrous acetonitrile. Polymerization was initiated on the surface of platinum disk electrode by repeated potential scans between 1.00 V and 0.83 V, inducing a homogenous growth of an electroactive polymer film on the electrode. Then the polymers were very quickly deposited on gold at a constant potential and deposition charge. θ_{CA} measurements indicated that the polymeric surfaces are both superhydrophobic (θ_{CA} = 161° for water) and superoleophobic (θ_{CA} = 145° for hexadecane, Fig. 10d). SEM images revealed that the surface morphology consists of a very porous material at a nanometric scale and an assembly of spherical structures at a micrometric scale (Figs. 10b and 10c). This two-scale construction enables the surface with exceptional super-antiwetting properties because it allows the surface to trap air beneath the surface, which supports the weight of a water/oil droplet more easily. In their subsequent works,[69,70] the authors found that the length of the alkylenedioxy bridge of the fluorinated 3,4-alkylenedioxypyrrole monomer plays a considerable important role in the surface morphology of the electrodeposited conducting polymer film: the polymerization of the fluorinated 3,4-ethylenedioxypyrrole monomer imparts the polymeric film with superamphiphobicity with extremely low CAH, whereas the polymerization of the fluorinated 3,4-propylenedioxypyrrole monomer gives only superhydrophobic films with sticking property (θ_{SA} > 90°). The different wettability was attributed to the presence of nanoporosity in fluorinated poly(3,4-ethylenedioxypyrrole) films, which increases both oil and water θ_{CA} and switches the system from the Wenzel to the Cassie–Baxter state. Very recently, the same group found that the surface microstructuration increases with the fluorinated-alkyl chain length, whereas the surface nanoporosity goes the reversed way.[71]

4. Functional applications

With the increasing demand for functional materials with excellent anti-wetting ability, a great deal of interest has been focused on the development of superamphiphobic surfaces displaying a wide range of applications.[5,9] The discussion below will focus on how surface superamphiphobic modification brings about new functions such as super-antiwetting, self-cleaning, anti-freezing, anti-bacteria, corrosion resistance, oil droplets manipulation, to name but a few, which are not available for the materials themselves.

4.1. Super-antiwetting

There is no doubt that the most applications of superamphiphobic surfaces are based on their versatile function in super-antiwetting, and all the other applications are derived from such a basic function. Superamphiphobic surfaces display characteristics of both superhydrophobic and superoleophobic, and thereby they share most of the functions with superhydrophobic surfaces with some exceptions. For instance, superhydrophobic surfaces can normally be used for oil/water separation because these super-water-repellent surfaces are wettable by low surface tension oils;[7] however, it is obvious that superamphiphobic surfaces cannot be used in such an application. However, compared with superhydrophobic surfaces, the biggest advantage of superamphiphobic surfaces is their super-antiwetting ability not only for pure water but also for low surface tension aqueous solution (for *e.g.*, detergent solution, rain water, underground water, waste water, and sea water.) and organic 'oils' (for *e.g.*, hexane, hexadecane, toluene, mineral oil, and cooking oil.).[9]

In Seeger's group, superamphiphobic coatings with super-antiwetting ability for both water and various low-surface tension organic liquids were prepared using silicone nanofilaments through a grow-from approach.[9] As mentioned above (section 3.1.1.1), with such a technique, a layer of SNF can be grown on various substrates by chemical deposition of trichloromethylsilane (TCMS) in the presence of water. The coated glass surfaces display super-antiwetting ability for probing liquid of water (θ_{CA} = 168 °, θ_{SA} = 5°), but not for low-surface-tension 'oils'.[9] For example, θ_{CA} for diiodomethane which shows

surface tension of 50.8 $mN \cdot m^{-1}$ is 91°; other 'oils' such as mineral oil, toluene, cyclohexane, hexadecane and decane which exhibit surface tension between 32 $mN \cdot m^{-1}$ and 23 $mN \cdot m^{-1}$ can spread on the surface quickly ($\theta_{CA} \approx 0°$), indicating that these samples are superoleophilic. Such coatings (on textile substrates) can be used for oil/water separation due to their superhydrophobicity but superoleophilicity.[72] Upon activating by O_2 plasma and surface modifying with PFDTS, the coatings show superamphiphobicity and cannot be wetted by both water and low surface tension 'oils' (Fig. 11a). For all of the liquids mentioned above, a high θ_{CA} (> 155°) and low θ_{SA} (< 6°) on the coated glass surface was observed, indicating that all of the liquid droplets on such a surface are in the Cassie–Baxter state. The liquid droplets could easily roll off from the surface while it is slightly tilted (< 6°). Even jets of toluene and decane could bounce off the TCMS/PFDTS coated surface without leaving a trace (Fig. 11b). The TCMS/PFDTS-coated glass surface was reflective in toluene and remained completely dry after taken out (Fig. 11c), implying the existence of an air cushion between the solid surface and the liquids. This means that most of the area beneath the liquid droplet is a liquid–vapour interface, and thereby the interaction between the liquid and the coating is extremely weak. Compared with superhydrophobic surfaces, superamphiphobic surfaces are more useful in antiwetting for practical applications since the former surfaces can be easily contaminated by oily substances when the surfaces are exposed to an industrial or household environment and gradually lose their superhydrophobicity, while the later surfaces cannot be contaminated (Fig. 11) and their superamphiphobicity can maintain for a long time.

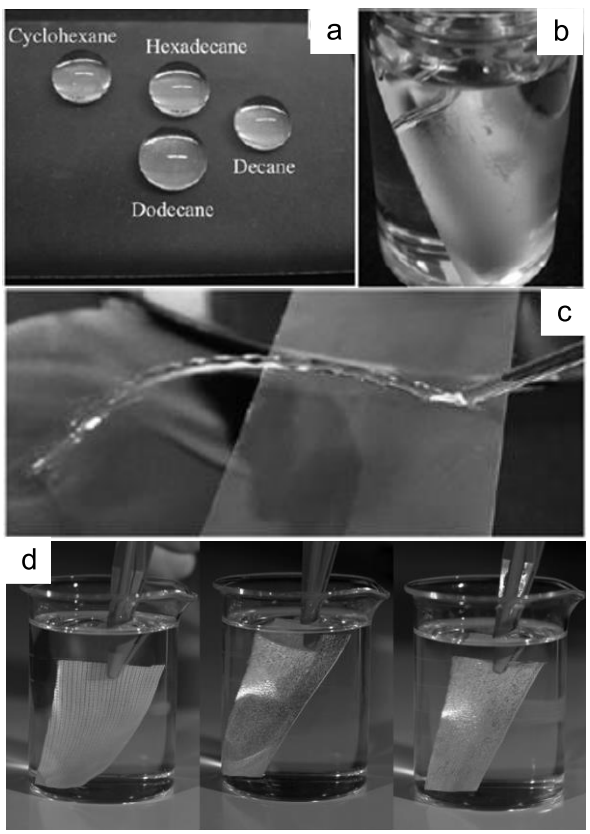

Fig. 11 Images of the superamphiphobic glass slides with droplets of various nonpolar liquids (a), immersed in toluene (b), and with a jet of toluene bouncing off (c), and untreated polyester fabric immersed in hexadecane (left), superamphiphobic fabric immersed in hexadecane (middle) and heptane (right). Figs. 11a–c were reproduced from ref. 9, copyright Wiley 2011. Fig. 11d was reproduced from ref. Reprinted with permission from ref. 53, copyright Elsevier 2012.

The super-antiwetting function can be applied to many traditional materials such as glass,[9,25,46,56], silicon,[5,7,42,43,55] zinc,[6,50] aluminium,[6,33] iron,[6] steel,[60] copper,[34,63] nickel,[6] engineering metal alloys,[6] textile,[23,53] polyester fabric,[61] paper,[62] gel,[51,52] and so on, protecting their surfaces from being wetted, contaminated or fouled by water and oily pollutant. Besides, the surface superamphiphobic modification brings about not only super-antiwetting function but also other derived functions such as self-cleaning, anti-fogging, anti-bacteria, corrosion resistance, and oil transportation, which will be discussed in the following sections.

4.2. Self-cleaning

Self-cleaning coatings can be broadly classified into two major types: photocatalysis-induced superhydrophilic coatings and superhydrophobic or superamphiphobic coatings.[47] In superhydrophilic coatings ($\theta_{CA} < 5°$), the surface is cleaned by the sheeting effect of water and also by breaking down the complex organic substances into carbon dioxide and water – the photocatalytic effect. On the contrary, in superhydrophobic or superamphiphobic surfaces, the air pockets that get trapped between nanostructured substrate and the water droplet result in the formation of a composite solid/air/liquid interface, which leads to an increase in θ_{CA} of liquid droplet, and thereby facilitating the de-wetting of the surface and enabling the droplet to roll-off easily, taking away the dirt and other pollutants.[46,47]

4.3. Anti-freezing

Anti-freezing on material surface has long been a technological challenge because some outdoor infrastructures and high-technological devices such as aviation, space flight and radar can be easily affected or even destroyed by the large amount of adherent ice. For instance, supercooled water vapour and clouds in the upper-air layers can easily condense and subsequently freeze on aircraft surfaces during a flight, which results in the worst case in a dramatic decrease of the ascending force and may lead to an airplane's crash, *e.g.*, on October 31, 1994, when American Eagle Flight 4184 crashed because of ice formation on the wings after flying into icing conditions.

Surface superhydrophobic modification shows great potential to address such a challenge. Quéré *et al.*[73] demonstrated that freezing could remarkably be delayed when water droplets were deposited on cold superhydrophobic surfaces. It was reported that the presence of microtextures dramatically delay the freezing time of the water drops, by a factor between 3 and 5. Water droplets rolled off the cold superhydrophobic surface quickly without freezing. In contrast, drops on untreated surface spread quickly and formed a thin film on the surface, which was freezed immediately. The authors pointed out that the air sublayer in a superhydrophobic surface could provide substantial thermal insulation and thus delayed the freezing process. In the work by Song *et al.*,[74] it was observed that the presence of micro/nanostructural and chemical patterns are very important for the controlling of coalescing of microdroplets as well as their

quick self-removal. Kulinich and Farzaneh[75] discovered that CAH plays an important role in anti-freezing and a lower CAH normally contribute to a much longer delay of freezing time.[73,75]

Compared with superhydrophobic surfaces, superamphiphobic surfaces normally exhibit much lower water CAH (θ_{SA} close to 1° or even lower), as documented extensively.[9,25,46,47,60] Therefore, superamphiphobic surfaces are more promising in anti-freezing though the corresponding study in such an application for superamphiphobic surfaces has not yet been reported.

4.4. Anti-bacterial growth properties

In addition to extremely non-wettability, superamphiphobic surfaces also exhibit antibacterial activity.[76–78] Vilčnik *et al.*[76,77] investigated the antibacterial properties of hydrophobic–oleophobic sol–gel coatings for cotton fabrics by using Escherichia coli bacteria as a model, and found that superamphiphobic surfaces exhibited a long lasting antibacterial effect without the addition of any antibacterial agents. Antibacterial activity test revealed that the reduction of the bacteria on superamphiphobic cotton fabrics was nearly 100%.[77] In Huang's group,[78] superamphiphobic cellulose (commercial filter paper) was fabricated by chemical etching using alkaline solution to enhance the surface roughness, followed by depositing an ultrathin titania films *via* a facile surface sol–gel process, and subsequently surface modifying using *1H,1H,2H,2H*-perfluorooctyl trimethoxysilane (PFOTMS). Due to the combined surface roughness and low surface energy of the PFOTMS monolayers, the naturally hydrophilic filter paper was converted into superamphiphobic, which effectively inhibited the adhesion of bacteria such as lysogenic Escherichia coli.

4.5. Corrosion resistance

The oxidation and corrosion of metals and their alloys in the humid atmosphere limit their applications, causing serious problems such as accelerated aging of the devices, huge waste, and environmental contamination.[79] Surface superamphiphobic modification is a probable solution to these problems because the super-repellent coating acts as durable barrier film that can effectively prevent the metal surface from being corroded. Recently, a superamphiphobic CaLi-based bulk metallic galss,[41] which was prepared by the construction of micro/nanoscale hierarchical structures and subsequent fluorination, was reported to show long-term stable anti-corrode ability due to its durable superamphiphobicity that can be kept in ambient atmospheric conditions for more than three months. In Jiang's group,[8,63] engineering metal and their alloys such as zinc, aluminium, iron, nickel and Zn/Fe alloy are superamphiphobic-functionalized by taking advantage of an electrochemical reaction in perfluorocarboxylic acid solution, which shows great promising in corrosion resistance for real applications since these metals are the most important and applicable materials in industry. In the work performed by Zhang *et al.*,[33] superamphiphobic aluminium was prepared in a facile way of HCl etcing, followed by PFOA surface modifying. In another study by the same research group,[80] superamphiphobic copper sheets were fabricated *via* a simple and time-saving procedure: sandblasting and Ag deposition process was used to create surface roughness firstly, and then the resultant surfaces were fluorinated by simple immersing the samples in PFDSH/ethanol solution (1 mM) for only 30 s. The obtained superamphiphobic surfaces exhibited enhanced corrosion resistance with a more positive corrosion potential and a more negative corrosion current density. More interestingly, the superamphiphobicity could be restored by a simple regeneration process when loss of superoleophobicity occurred. The authors suggested that such a simple and time-saving fabrication technique will make it possible for large-scale production of superamphiphobic engineering materials. Very recently, Tuteja and coworkers[60] developed superamphiphobic stainless steel wire meshes by electrospinning a blend of cross-linked poly(dimethylsiloxane) and FD-POSS. It was observed that the coated steel surface cannot be corroded by concentrated hydrochloric acid and concentrated sodium hydroxide.

4.6. Oil droplets manipulation

Recently, utilizing superamphiphobic surfaces with controllable oil adhesion, Jiang and coworkers constructed an oil droplet-based microreactor for oil droplets manipulation.[35] The surface adhesion to oil can be tuned through the adjustment of either surface nanostructures or external preload forces, making it possible for oil transportation in a drop-to-drop system. In their experiment, an oil droplet containing styrene monomer was transferred from a low adhesive superamphiphobic surface to a metal cap, which was then reacted with another oil droplet containing Br_2 on a high adhesion superamphiphobic surface. After the reaction of the two droplets, the final droplet was left on the substrate due to the high adhesion to the surface. These surfaces with controllable oil adhesion displayed promising applications in microfluidic systems, no-loss oil droplet transportation, and other fields.

4.7. Other applications

Except the functional applications discussed above, superamphiphobic surfaces also exhibit great potential in a variety of other fields including breathable protective wear,[23] enhanced solvent resistance,[9] chemical shelding,[60] drag reducing,[81] patterned superfunctional surfaces,[15] and smart devices[51], anti-reflection, and oil capture.

5. Conclusions and perspectives

This tutorial review summarizes the characterization, fabrication, and functional applications of superamphiphobic surfaces. The development of such surfaces is important for basic research, as well as, for numerous commercial applications. Through years of endless efforts, great achievements have been made in this field: a variety of different techniques towards the fabrication of superamphiphobic surface have been developed by combining design of surface roughness and surface chemistry. Nevertheless, there are still lots of challenges that need to be addressed. For example, a majority of the fabrication methods are limited to laboratory research and not suitable for industrial scale production. Even though the superamphiphobic coatings can be prepared in large scale, they generally face the problem of poor mechanical stability. Mechanical durability is crucial to practical applications, *i.e.*, they cannot find practical use without sufficient mechanical stability. However, this aspect has been sparingly addressed in literature and there is a need and an opportunity to develop mechanically durable superamphiphobic surfaces. The

relationship between mechanical stability and surface morphology as well as surface chemistry needs to be investigated. Quantitative ways to characterize the mechanical stability of superamphiphobic coatings should be established—there probably be a critical force above which the superamphiphobicity of the surface decreases substantially and methods for precise determination of such a critical force needs to be figured out.

Future trends in this field may see an expansion towards self-healing superamphiphobicity because it shows great promising in practical applications—their oil-repellency can easily be automatically restored after mechanical damage. Surfaces with controllable superamphiphobicity may also become one of the focuses of future research, given biological relevance of most of them.

Overall, we believe that an exciting future for superamphiphobic surfaces will be witnessed since many scientists and engineers contribute to the understanding and the design of such surfaces.

Acknowledgements

Financial support from University of Zurich and Swiss National Science Foundation (SNSF) is greatly acknowledged.

Notes and references

Department of Chemistry, University of Zurich, Zurich CH-8057, Switzerland. Tel.: + 41 (0) 44 6354 451; Fax: + 41 (0) 44 6356 813; E-mail: sseeger@pci.uzh.ch

1 H. Ollivier, *Ann. Chim. Phys.*, 1907, **10**, 229–288.
2 W. Barthlott C. and Neihuis, *Planta*, 1997, **202**, 1–8.
3 X. Zhang, F. Shi, J. Niu, Y. Jiang and Z. Wang, *J. Mater. Chem.*, 2008, **18**, 621–633, and references therein.
4 M. Liu, Y. Zheng, J. Zhai and L. Jiang, *Acc. Chem. Res.*, 2010, **43**, 368–377.
5 A. Tuteja, W. Choi, M. L. Ma, J. M. Mabry, S. A. Mazzella, G. C. Rutledge, G. H. McKinley and R. E. Cohen, *Science*, 2007, **318**, 1618–1622.
6 H. F. Meng, S. T. Wang, J. M. Xi, Z. Y. Tang and L.Jiang, *J. Phys. Chem. C*, 2008, **112**, 11454–11458.
7 A. Tuteja, W. Choi, J. M. Mabry, G. H. McKinley and R. E. Cohen, *Proc. Natl. Acad. Sci. USA*, 2008, **105**, 18200–18205.
8 T. Darmanin and Guittard, *Langmuir*, 2009, **25**, 5463–5466.
9 J. Zhang and S. Seeger, *Angew. Chem., Int. Ed.*, 2011, **50**, 6652–6656.
10 H.-J. Butt, C. Semprebon, P. Papadopoulos, D. Vollmer, M. Brinkmann and Matteo Ciccotti, *Soft Matter*, 2013, **9**, 418–428.
11 J. Genzer and K. Efimenko, *Biofouling*, 2006, **22**, 339–360.
12 R. N. Wenzel, *Ind. Eng. Chem.*, 1936, **28**, 988–994.
13 A. B. D. Cassie and S. Baxter, *Trans. Faraday Soc.*, 1944, **40**, 546–551.
14 J. Zimmermann, S. Seeger and F. A. Reifler, *Text. Res. J.*, 2009, **79**, 1565–1570.
15 J. Zimmermann, M. Rabe, G. R. J. Artus and S. Seeger, *Soft Mater*, 2008, **4**, 450–452.
16 L. Cao, T. P. Price, M. Weiss and D. Gao, *Langmuir*, 2008, **24**, 1640–1643.
17 H. J. Li, X. B. Wang, Y. L. Song, Y. Q. Liu, Q. S. Li, L. Jiang and D. B. Zhu, *Angew. Chem., Int. Ed.*, 2001, **40**, 1743–1746.
18 K.-H. Cho and L.-J. Chen, *Nanotechnology*, 2011, **22**, 445706, and reference therein.
19 G. R. J. Artus, S. Jung, J. Zimmermann, H.-P. Gautschi, K. Marquardt and S. Seeger, *Adv. Mater.*, 2006, **18**, 2725–2762.
20 T.-S. Wong, S. H. Kang, S. K.Y. Tang, E. J. Smythe, B. D. Hatton, A. Grinthal and J. Aiyenberg, *Nature*, 2011, **477**, 443–447.
21 Y. Huang, J. Zhou, B. Su, L. Shi, J. Wang, S. Chen, L. Wang, J. Zi, Y. Song and L. Jiang, *J. Am. Chem. Soc.*, 2012, **134**, 17053–17058.
22 M. Kuang, J. Wang, B. Bao, F. Li, L. Wang, L. Jiang and Y. Song, *Adv. Opt. Mater.*, 2014, DOI: 10.1002/adom.201300369.
23 B. Leng, Z. Shao, G. de With and W. Ming, *Langmuir*, 2009, **25**, 2456–2460.
24 C.-T. Hsieh, F.-L. Wu and W.-Y. Chen, *Mater. Chem. Phys.*, 2010, 121, 14–21.
25 Z. He, M. Ma, X. Lan, F. Chen, K. Wang, H. Deng, Q. Zhang and Q. Fu, *Soft Matter*, 2011, **7**, 6435–6443.
26 C.-F. Wang, W.-Y. Chen, H.-Z Cheng and S.-L. Fu, *J. Phys. Chem. C*, 2010, **114**, 15607–15611, and references therein.
27 M. Zhang, T. Zhang and T. Cui, *Langmuir*, 2011, **27**, 9295–9301.
28 A. Das, T. M. Schutzius, I. S. Bayer and C. M. Megaridis, *Carbon*, 2012, **50**, 1346–1354.
29 J. Zimmermann, S. Seeger, G. Artus and S. Jung, WO 2004113456, **2004**.
30 J. Zimmermann, F. A. Reifler, G. Fortunato, L.-C. Gerhardt and S. Seeger, *Adv. Funct. Mater.*, 2008, **18**, 3662–3669.
31 J. Zimmermann, G. R. J. Artus and S. Seeger, *Appl. Surf. Sci.*, 2007, **253**,5972–5979.
32 J. Zimmermann, F. A. Reifler, U. Schrade, G. R. J. Artus and S. Seeger, *Colloids Surf. A*, 2007, **302**, 234–240.
33 J. Yang, Z. Zhang, X. Xu, X. Men, X. Zhu and X. Zhou, *New J. Chem.*, 2011, **35**, 2422–2426.
34 X. Zhu, Z. Zhang, X. Xu, X. Mena, J. Yang, X. Zhou and Q. Xue, *J. Colloid Interface Sci.*, 2012, **367**, 443–449.
35 X. Yao, Y. Song and L. Jiang, *Adv. Funct. Mater.*, 2011, **21**, 4270–4276.
36 H. Kim, K. Noh, C. Choi, J. Khamwannah, D. Villwock and S. Jin, *Langmuir*, 2011, **27**, 10191–10196.
37 L. Cao, T. P. Price, M. Weiss and D. Gao, *Langmuir*, 2008, **24**, 1640–1643.
38 Y. Liu, Y. Xiu, D. W. Hess and C. P. Wong, *Langmuir*, 2010, **26**, 8908–8913.
39 S. M. Ramos, A. Benyagoub, B. Canut and C. Jamois, *Langmuir*, 2010, **26**, 5141–5146.
40 C. Aulin, S. H. Yun, L. Wågber and T. Lindström, *Acs. App. Mater. Interface*, 2009, **1**, 2443–2452.
41 K. Zhao, K. S. Liu, J. F. Li, W. H. Wang and L. Jiang, *Scripta Mater.*, 2009, **60**, 225–227.
42 H. Zhao, K.-Y. Law and V. Sambhy, *Langmuir*, 2011, **27**, 5927–5935.
43 H. Zhao and K.-Y. Law, *Langmuir*, 2012, **28**, 11821–11827.
44 M. Im, H. Im, J.-H. Lee, J.-B. Yoon and Y.-K. Choi, *Soft Matter*, 2010, **6**, 1401–1404.
45 A. Susarrey-Arce, Á. G. Marín, L. Lefferts, J. G. E. Gardeniers and A. von Houselt, *J. Micromech. Microeng.*, 2013, **23**, 025004.
46 X. Deng, L. Mannen, H.-J. Butt and D. Vollmer, *Science*, 2012, **335**, 67–70.
47 V. A. Ganesh, S. S. Dinachali, H. K. Raut, T. M. Walsh, A. S. Nair and S. Ramakrishna, *RSC Advance*, 2013, **3**, 3819–3824.
48 T. Fujii, Y. Aoki and H. Habazaki, *Langmuir*, 2011, **27**, 11752–11756.
49 T. Fujii, H. Sato, E. Tsuji, Y. Aoki and H. Habazaki, *J. Phys. Chem. C*, 2012, **116**, 23308–23314.
50 X. Xu, Z. Zhang, F. Guo, J. Yang, X. Zhu, X. Zhou and Q. Xue, *Colloid Surf. A.*, 2012, **396**, 90–95.
51 H. Jin, M. Kettunen, A. Laiho, H. Pynnönen, J. Paltakari, A. Marmur, O. Ikkala and R. H. A. Ras, *Langmuir*, 2011, **27**, 1930–1934.
52 H. Jin, X. Tian, O. Ikkala and R. H. A. Ras, *ACS Appl. Mater. Interfaces*, 2013, **5**, 485−488.
53 G. R. J. Artus, J. Zimmermann, F. A. Reifler, S. A. Brewer and S. Seeger, *App. Surf. Sci.*, 2012, **258**, 3835–3840.
54 Y.-C. Sheen, Y.-C. Huang, C.-S. Liao, H.-Y. Chou and F.-C. Chang, *J. Polym. Sci. B: Polym. Phys.*, 2008, **46**, 1984–1990.
55 R. Campos, A. J. Guenthner, A. J. Meuler,A. Tuteja,R. E. Cohen, G. H. McKinley, T. S. Haddad and J. M. Mabry, *Langmuir*, 2012, **28**, 9834–9841.
56 X. Wang, H. Hu, Q. Ye, T. Gao, F. Zhou and Q. Xue, *J. Mater. Chem.*, 2012, **22**, 9624–9631.

57 J. Yang, Z. Zhang, X. Men, X. Xu and X. Zhu, *New J. Chem.*, 2011, **35**, 576–580.
58 D. Han and A. J. Steckl, *Langmuir*, 2009, **25**, 9454–9462.
59 S. Srinivasan, S. S. Chhatre, J. M. Mabry and R. E. Cohen, *Polymer*, 2011, **52**, 3209–3218.
60 S. Pan, A. K. Kota,J. M. Mabry and A. Tuteja, *J. Am. Chem. Soc.*, 2013, **135**, 578−581.
61 H. Wang, Y. Xue, J. Deng, L. Feng, X. Wang and T. Lin, *Angew. Chem., Int. Ed.*, 2011, **50**, 11433–11436.
62 D. Xiong, G. Liu and L. Hong, *Chem. Mater.*, 2011, **23**, 4357–4366.
63 J. Xi, L. Feng and L. Jiang, *Appl. Phys. Lett.*, 2008, **92**, 053102.
64 H. Meng, S. Wang, J. Xi, Z. Tang and L. Jiang, *J. Phys. Chem. C*, 2008, **112**, 11451–11458.
65 H. Wang, Y. Xue and T. Lin, *Soft Matter*, 2011, **7**, 8158–8161.
66 H. Wang, H. Zhou, A. Gestos, J. Fang, H. Niu, J. Ding and T. Lin, *Soft Matter*, 2013, **9**, 277–282.
67 R. Saraf, H. J. Lee, S. Michielsen, J. Owens, C. Willis, C. Stone and E. Wiluzs, *J. Mater. Sci.*, 2011, **46**, 5751–5760.
68 T. Darmanin and F. Guittard, *J .Colloid and Interface Sci.*, 2009, **335**, 146–149.
69 T. Darmanin and F. Guittard, *Chem. Commun.*, 2009, 2210–2211.
70 T. Darmanin and F. Guittard, *J. Am. Chem. Soc.*, 2009, **131**, 7928–7933.
71 H. Bellanger, T. Darmanin and F. Guittard, *Langmuir*, 2012, **28**, 186–192.
72 J. Zhang and S. Seeger, *Adv. Funct. Mater.*, 2011, **21**, 4699–4704.
73 P. Tourkine , M. Le Merrer and D. Quéré , *Langmuir*, 2009 , **25** , 7214–7216 .
74 M. He, Q. Zhang, X. Zeng, D. Cui, J. Chen, H. Li, J. Wang and Y. Song, *Adv Mater.*, 2013, **25**, 2291–2295.
75 S. A. Kulinich and M. Farzaneh , *Appl. Surf. Sci.*, 2009 , **255** , 8153–8157.
76 B. Tomšič, B. Simončič, B. Orel, L. Černe, P. F. Tavčer, M. Zorko, I. Jerman, A. Vilčnik and J. Kovač, *J. Sol–Gel Sci. Technol.*, 2008, 47, 44–57.
77 A. Vilčnik, I. Jerman, A. S. Vuk, M. Koželj, B. Orel, B. Tomšič, B. Simončič and J. Kovač, *Langmuir*, 2009, **25**, 5869–5880.
78 C. Jin, Y. Jiang, T. Niu and J. Huang, *J. Mater. Chem.*, 2012, **22**, 12562–12567.
79 X. Yao, Y. Song and L. Jiang, *Adv. Mater.*, 2011, **23**, 719–734.
80 Z. Zhang, X. Zhu, J. Yang, X. Xu, X. Meng and Z. Zhou, *Appl. Phys. A*, 2012, **108**, 601–606.
81 C. Lee and C.-J. Kim, *Phys. Rev. Lett.*, 2011, **106**, 014502.

Author biographies

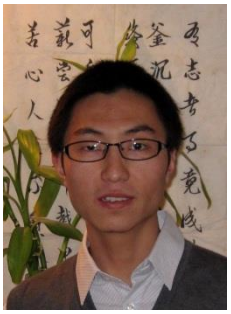

Dr Zonglin Chu earned his BSc in Applied Chemistry from Hunan University, China, in 2006, joined Prof. Yujun Feng's group as a Master-to-Ph.D student at Chengdu Institute of Organic Chemistry, Chinese Academy of Sciences the same year, and received his PhD in Chemical Engineering in 2011. His PhD project in the field of alkylamidosulfobetaine wormlike micelles and stimuli-responsive worms resulted in more than 10 publications in high impact factor journals. After one year of postdoctoral research in multi-step organic synthesis in the Lab of Organic Chemistry, ETH Zürich, he is currently working on superamphiphobic surfaces in Prof. Dr Stefan Seeger's group in the Department of Chemistry, University of Zurich. His research interests lie at the interface of organic synthesis, colloid and interface science, hydrogels, smart materials, and functional surfaces with special wettability.

.

Stefan Seeger studied chemistry at the Ruprecht Karl University of Heidelberg and at the Technical University of Berlin. In 1992 he attained a doctorate in chemistry in Heidelberg. Subsequently, Stefan Seeger led the Department of Biophysical Chemistry at the Physicochemical Institute at the University of Heidelberg, where he was appointed a scientific assistant later. Between 1988 and 1992 he studied marketing and management at the University of Hagen. 1995 followed a six month's research stay at the Chemical Center of the University of Lund, Sweden. One year later he attained his habilitation in Heidelberg and in summer 1997 he was appointed as a professor for biochemistry and bio sensor technology at the University of Regensburg. In November 1999 Stefan Seeger was appointed as a professor for physical chemistry at the University of Zurich.